Comparison of resonant magnetic perturbation induced particle transport changes in H-mode (DIII-D) and L-mode (MAST)

S Mordijck[1], R A Moyer[2], A Kirk[3], P Tamain[4], D Temple[3], G R McKee[5] and E Nardon[4]

[1] The College of William and Mary, McGlothlin-Street Hall, Williamsburg, Virginia 23187, USA
[2] University of California-San Diego, 9500 Gilman Dr., La Jolla, California 92093, USA
[3] EURATOM/CCFE Fusion Association, Culham Science Centre, Abingdon, OX14 3DB, UK
[4] CEA, Cadarache, 13108 St Paule lez Durance Cedex, France
[5] University of Wisconsin-Madison, Madison, Wisconsin 53706

E-mail: mordijck@cs.wm.edu

Abstract. Recent experiments show the impact of Resonant Magnetic Perturbations on the density [O Schmitz *et al* Plasma Phys. Control. Fusion **50** 124029 (2008); T E Evans *et al* Nucl. Fusion **48** 024002 (2008); A Kirk *et al* Nucl. Fusion **50** 024002 (2008); Y Liang *et al* Phys. Rev. Lett. **98** 265004 (2007)], leading to a so-called density pump-out. Previous comparisons between DIII-D and TEXTOR have focussed on the similarities of the deformation of the separatrix and the creation of striations at the intersection of the main chamber wall [O Schmitz *et al* Plasma Phys. Control Fusion **50** 124029 (2008); O Schmitz *et al* Phys. Rev. Lett. **103** 165005 (2009)]. In this paper, we compare the difference in magnitude of the experimentally observed density pump-out in L-mode with H-mode in two diverted tokamaks: MAST and DIII-D. In order to address the differences in magnetic field from the coils, plasma shape and q_{95} between the two devices, we compute a weighted magnetic diffusion coefficient with a vacuum field line tracing code. This allows us to compare the changes in density pump-out with the weighted magnetic diffusion coefficient, using a simple particle diffusion model. We find that the density pump-out is vastly different in the two devices, suggesting different

particle transport mechanisms. Since one main difference in transport characterics between L- and H-mode is turbulence, we compare turbulent particle characteristics. We find that in L-mode (MAST) the fluctuations and $E \times B$ shear increase at the plasma edge, whereas in H-mode (DIII-D) the fluctuations decrease at the plasma edge. Deeper inside the core, the $E \times B$ shear remains similar in L-mode (MAST), whereas a large decrease that quickly saturates with RMP strength is observed in H-mode (DIII-D). These results suggest that the RMP induced particle transport at the plasma edge in L-mode (MAST) is the result from increases in turbulent particle transport, whereas the results in H-mode (DIII-D) suggest a decrease in turbulent particle transport.

PACS numbers: 52.25.Fi Transport properties, 52.35.Ra Plasma Turbulence, 52.55 Tokamaks, spherical tokamaks

Submitted to: *Plasma Phys. Control. Fusion*

1. Introduction

Resonant magnetic perturbations (RMPs) are a successful technique to suppress edge-localized modes (ELMs) [1], which can erode divertor materials in future tokamak devices due to high impulsive heat fluxes [2]. In DIII-D, RMPs eliminate ELMs by reducing the pedestal pressure gradient below the peeling-ballooning stability limit [3], by increasing particle transport [4, 5, 6] and reducing the pedestal density. This density pump-out ranges from 5% to 30% as a fraction of the line average density in ELMing H-mode prior to RMP-coil application. It is critical to limit this density pump-out to the minimum level needed to achieve ELM suppression in order to minimize the impact of RMP ELM suppression on plasma performance in ITER.

In order to understand how RMPs are related to the density pump-out and to make confident predictions for ITER, we need to compare how particle transport in different experimental devices with ITER-like coils is affected by RMPs. In this paper, we investigate the impact of turbulent transport and $E \times B$ shear, $\omega_{E\times B}$, changes on density pump-out by comparing RMP L- and H-mode data from two diverted tokamaks that have two rows of six off-midplane internal picture frame coils that produce $n = 3$ toroidal mode number RMPs: DIII-D and MAST. Both tokamaks are the only ones that are capable of an $n = 3$ spectrum with internal picture frame coils. Where DIII-D has a large dataset of RMP H-modes in ITER-similar shape (ISS) and $\nu^* \sim 0.1$ pedestal collisionality, MAST has a large dataset on density pump-out with RMP in Connected Double Null (CDN) L-modes and a collisionality larger than $\nu^* > 1$ [7].

Previous machine comparisons between DIII-D and TEXTOR have focused on the creation of tangle structures on the limiter or divertor target plates [8, 9]. Both machines clearly show the formation of striations in the strike-point, although their coil configuration, magnetic spectra and confinement, plasma shape and divertor versus limiter configuration are vastly different. The location of these experimentally observed tangles agree well with simulation of the vacuum magnetic field line topology for both experimental devices. Therefore, to investigate the changes in particle transport as

a result of RMPs at the plasma edge, we introduce a weighted magnetic diffusion coefficient, D_{OFL} and a simple particle balance model (section 2.1). This allows us to incorporate the differences in plasma shape, spectrum, q_{95} on RMP-induced particle transport between MAST and DIII-D RMP experiments. Consequently, we can now compare the magnitude of the density pump-out as a result of RMPs in both machines.

The density pump-out in MAST L-modes (MAST) is much smaller for a similar weighted diffusion coefficient, D_{OFL} than in H-modes (DIII-D). One obvious difference between H-mode and L-mode is the reduction in turbulent transport in the H-mode pedestal due to $E \times B$ shear suppression [10]. Therefore, we investigate the changes in $E \times B$ shearing rate measured by charge exchange recombination spectroscopy (CER) [11] and the normalized rms density fluctuations levels $\tilde{n}/n$ from long wave-length fluctuations ($k_\theta \sim 1\,\mathrm{cm}^{-1}$) to determine if changes to ion-scale turbulent transport can explain the differences we observe in density pump-out between the MAST L-mode (MAST) and H-mode (DIII-D) RMP discharges.

In H-mode (DIII-D), RMP decreases the $E \times B$ shear for $0.7 \leq \Psi_N \leq 0.9$; this decrease saturates even at the lowest applied I-coil current (4 kA) in this series of experiments (section 3.1). Another aspect of changes to turbulent transport is the increase in normalized density fluctuations at the ion scale $k_\theta \sim 1\,\mathrm{cm}^{-1}$ with increasing RMP-coil current at $\Psi_N = 0.88$, which agrees with previous work [6, 12]. In contrast, at $\Psi_N = 0.95$, $\tilde{n}/n$ decreases with increasing RMP-coil current except at the highest RMP-coil current, which is also different from previous work on $\nu^* > 1$ RMP discharges, where the intermittent behavior of the turbulence increases when the ELMs are suppressed [13].

In L-mode (MAST), $E \times B$ does not change in the region $0.85 \leq \Psi_N \leq 0.92$ (section 3.2). Outside $\Psi_N > 0.92$, measurements with the fast reciprocating probe indicate that the E_r well becomes more positive [14]. This paper shows that the rms ion saturation current fluctuations $\tilde{I}_{SAT}$ [with I_{SAT} proportional to $n(T_e + T_i)^{1/2}$] increase inside the seperatrix.

2. Comparison of Density Pump-out

In this section we introduce a simple particle balance model to compare changes to the particle transport by RMPs with changes in electron density. Subsequently, we introduce the calculation of the weighted magnetic diffusion coefficient (D_{OFL}) to represent the increase in particle transport as a result of RMPs. Using D_{OFL} allows us to incorporate changes to the shape, q-profile, spectrum, devices and divertor configuration. Finally we compare the density pump-out in H-mode (DIII-D) with L-mode (MAST) using D_{OFL} and the simple particle balance model.

2.1. Particle balance model

To compare the L-mode and H-mode data, we use a simple particle balance for steady-state, and set the particle source S equal to the integral of the diffusive flux across the last closed flux surface (LCFS):

$$\oint D\nabla n \cdot dA = S \quad . \tag{1}$$

Here D is the effective diffusion coefficient and n is the electron density. For a characteristic density gradient length $l = n/\nabla n$ and by taking the integral we can rewrite equation (1) as:

$$Dn = \frac{Sl}{A} \quad . \tag{2}$$

In the experiments discussed in this paper, we can assume that the right-hand side of equation (2) remains constant from the reference experiment when compared to the RMP experiments. The neutral beam or gas puff fueling in these experiments is similar, the area of the separatrix is not altered and the characteristic density gradient at the separatrix remains fairly constant. Therefore, the difference between a reference discharge and a RMP discharge is gradient of equation (2); i.e. $\Delta(Dn)_{shot} = 0$. With partial differentiation this leads to:

$$(\Delta n)_{shot} = \frac{n}{D}(\Delta D)_{shot} \quad . \tag{3}$$

From the experimental data, we can determine the $(\Delta n)_{shot}$ as the difference in electron density between a reference discharge without RMP-coil current and one with RMP-coil current. In the next section, we introduce the calculation of a weighted magnetic diffusion coefficient D_{OFL}, to represent $(\Delta D)_{shot}$ in equation (3).

2.2. Calculation of weighted magnetic diffusion coefficient

We test the assumption that the density pump-out is the direct consequence of the applied resonant magnetic perturbation. This means that the increase in transport can be directly related to the changes in magnetic topology, independent of the fact whether the magnetic topology leads directly to the density pump-out or indirectly (i.e. changes to laminar zone transport [15] versus changes in neoclassical transport [16]). As a result, employing a weighted magnetic diffusion coefficient to represent the changes in transport does not imply the transport change is the result of magnetic diffusion, it is only a measure to represent the influence of the vacuum field on the plasma edge.

We calculate the weighted diffusion coefficient, D_{OFL}, using TRIP3D, a vacuum field line integration code [17], that includes contributions from resonant and non-resonant components of the externally applied perturbation, error-fields (only known for DIII-D), and error-field correction. The calculation of D_{OFL} is based on the weighted magnetic field line diffusion coefficient D_M [18]. D_M has a radial profile and in order to simplify this radial profile to present an effective increase in transport across the LCFS, we integrate the value of D_M over $0.8 \leq \Psi_N \leq 1$, where Ψ_N is the normalized poloidal magnetic flux. Next, we subtract D_{OFL} of the reference case without any $n = 3$ RMP but including the effects of known error-fields (DIII-D only in this paper) and error field correction coils as shown in equation (4):

$$\Delta D_{OFL} = \frac{\Delta\Psi_n}{M}\left[\left(\sum_{j=1}^{M}\frac{N_{lost_j}}{N_j}\left(\frac{1}{N_j}\sum_{i=1}^{N_j}\frac{(\delta r_i)^2}{2L_i}\right]\right)_{RMP}\right.$$
$$\left.-\left(\sum_{j=1}^{M}\frac{N_{lost_j}}{N_j}\left[\frac{1}{N_j}\sum_{i=1}^{N_j}\frac{(\delta r_i)^2}{2L_i}\right]\right)_{non-RMP}\right] \quad . \tag{4}$$

Here, $\Delta\Psi_N$ is the range over which we sum the number of flux surfaces M. N is the number of field lines and N_{lost} is the number of field lines that hit the target plates. The summation over i is a sum over N_j field lines on the j^{th} flux surface, and the summation over j is over the M flux surfaces. δr is the radial movement of the field line from starting point to end point, mapped from Ψ_N space to real space at the outboard midplane and L is the total length of the field line. If the field line ends at the wall, this is the length used in the calculation, field lines that do not reach a wall before 200 toroidal rotations, are given the length they have at 200 toroidal rotations. The calculations include 180 field lines on each flux surface and 40 flux surfaces equally spaced over $0.8 \leq \Psi_N \leq 1$. ΔD_{OFL} has the units of meters and we multiply ΔD_{OFL} with the plasma sound speed c_s, as a characteristic velocity for particle transport in a plasma edge to obtain $(\Delta D)_{shot}$.

2.3. Comparison between H-mode (DIII-D) and L-mode (MAST)

In figure 1, we plot the density pump-out, Δn_e, versus the change in vacuum weighted diffusion coefficient ΔD_{OFL} by comparing the density in each RMP discharge to a matched non-RMP reference discharge. For L-mode (MAST), Δn_e is based on the line-averaged density; for H-mode (DIII-D), Δn_e is based on the change in electron density at the top of the pedestal.

The difference in Δn_e between H-mode (DIII-D) and (L-mode) MAST for a similar D_{OFL} coefficient and the differences in slope are discussed in section 4. The largest differences between the MAST and DIII-D RMP experiments is the confinement regime; i.e. L- versus H-mode. This leads to different particle transport regimes in the pre-RMP phase of the discharge, with one of the main differences the introduction of a strong $E\times B$ shearing barrier at the plasma edge in H-mode [10]. Therefore, we will investigate the

changes in turbulent transport characteristics resulting from RMPs in L-mode (MAST) and H-mode (DIII-D).

3. Experimental Turbulence Characteristics

3.1. ISS H-mode (DIII-D)

We restrict ourselves to changes in low collisionality H-mode plasmas, $\nu^* \leq 0.2$, in the ITER similar shape [19], which has an average triangularity of $\langle\delta\rangle \sim 0.53$, $I_p = 1.68$ MA, $B_T = 2.1\,\mathrm{T}$, $\beta_N \sim 2.0$ and $q_{95} = 3.6$. At 1800 ms, the two rows of internal off-midplane RMP-coils are energized in $n = 3$ even parity (upper and lower coils at the same toroidal angle have the same current direction) 60 deg phasing [18]. In the reference discharge with the RMP coil off, the density is still rising at 1800 ms [18]; we therefore compare the pedestal density of the RMP discharges to the reference discharge at 3000 ms.

Previous work [6] compared changes in radial electric field, E_r, and turbulence to changes in particle transport. It was shown that the E_r well in the H-mode pedestal narrows and toroidal rotation increases rapidly when the RMP is applied. This leads to a reduction in E_r shear inside $\Psi_N \approx 0.9$. At the same time $\tilde{n}$ measured by a coherent scattering system (not radially localized) [20] and a homodyne reflectometer (the reflection layer moves because the density pumps out) [6] increases when the RMP is applied, and increases further when the ELMs are suppressed.

In figure 2, we compare $\omega_{E\times B}$ at 3000 ms for $0.7 \leq \Psi_N \leq 0.9$ in steady state with the RMP applied. The $\omega_{E\times B}$ is reduced during the RMP-coil pulse for the lowest current (4 kA), and does not change significantly as the current is increased to 6.2 kA. This decrease in $E \times B$ shear suggests that particle transport in this region may increase due to reduced decorrelation of the turbulence. In the transport barrier ($\Psi_N \approx 0.95$), $\omega_{E\times B}$ generally increases when the RMP is applied, but there is no clear trend with increasing I-coil current.

We show the $\tilde{n}/n$ changes in figure 3 for two radii measured by beam emission spectroscopy [22] which measure localized, long wave-length ($k_\perp \rho_I < 1$) density

fluctuations. The first measurement is from $\Psi_N = 0.88$ (gray band in figure 2) inside the region where $\omega_{E\times B}$ is reduced (figure 3), which shows that ion-scale fluctuations increase with increasing RMP-coil current. The second measurement is from $\Psi_N = 0.95$ (red band in figure 2) in the pedestal. The $\tilde{n}/n$ fluctuations in the pedestal decrease with increasing RMP-coil current and the $\omega_{E\times B}$ increases for most RMP-coil currents, but does not correlate with the decrease in fluctuations. Only at the highest RMP-coil current are the fluctuations close to the levels for the reference discharge without the $n = 3$ RMP field.

3.2. CDN L-mode (MAST)

To assess the role of turbulent transport changes in the density pump-out, we compare the DIII-D H-mode results to Ohmic L-mode discharges in MAST with $I_p = 400\,\mathrm{kA}$, $B_T = 0.52\,\mathrm{T}$, $\beta \sim 0.7$, $\nu^* > 1$ and $q_{95} = 6$ [7]. The MAST RMP-coils are applied in even parity, producing a density pump-out [7] that scales linearly with increasing weighted diffusion coefficient, ΔD_{OFL} once a minimum RMP is reached (figure 1).

Contrary to the DIII-D results, $\omega_{E\times B}$ does not change when the RMP-coil is energized for $\Psi_N \leq 0.92$ as measured by Doppler spectroscopy using an outbboard helium gas puff. However, probe measurements of E_r show a clear change for $\Psi_N > 0.92$ [14]. However, both diagnostics agree that for $\Psi_N \leq 0.92$ $\omega_{E\times B}$ does not change when RMP is applied.

Tamain *et al* [14] show that the normalized $\tilde{I}_{SAT}$ fluctuations increase inside the last closed flux surface. The increase depends on the amount of RMP-coil current applied. For the lowest RMP-coil current, for which no density pump-out is observed, no increase in fluctuations is observed, consistent with the threshold RMP-current for pump-out in figure 1. However, at the highest RMP-coil current, the density is reduced and the fluctuations increase. This increase in the normalized $\tilde{I}_{SAT}$ fluctuations shows a similar threshold dependence on I-coil current, consistent with the E_r probe measurements. These changes in turbulent transport inside the separatrix are similar to moderate

collisionality ELM-suppressed H-modes in DIII-D [13].

4. Discussion and Conclusion

4.1. $E \times B$ shear DIII-D

In H-mode (DIII-D), the $E \times B$ shear decreases when the RMP is applied, suggesting that in the core turbulent transport increases due to a reduction in the $E \times B$ shear suppression. The large $\omega_{E\times B}$ change at the even lowest applied RMP current may be an example of a change in particle transport that is not correlated with D_{OFL} and could be part of the explanation of the large off-set observed for DIII-D H-mode data in figure 1.

4.2. Off-set in correlation

Based on the simple particle balance equation [equation (3)], the density pump-out should be directly correlated to a change in RMP, leading to a linear correlation passing through (0,0) with a slope of n/Dc_s, with c_s the plasma sound speed to change the units of D_{OFL} from m to m^2/s. The L-mode (MAST) data passes through zero, close to limits imposed by diagnostic accuracy (i.e. the offset is only -0.32×10^{18}). For H-mode (DIII-D) plasmas, the off-set (1×10^{19}) is well outside the accuracy limits of the diagnostic. The fact that the linear correlation is not passing through (0,0) means that the density pump-out in H-mode (DIII-D) plasmas does not correlate directly with the applied RMP. The offset can be explained by the fact that another transport channel is affected by the RMP, which does not scale with influence of RMP, as expressed with D_{OFL}, i.e., the parameter D_{OFL} does not capture all of the shear rate, which changes drastically from 0 to 4 kA, but remains fairly constant with increasing RMP current.

4.3. Slope of correlation

The slope of the linear correlation for L-mode (MAST) and H-mode (DIII-D) are different (figure 1). Based on the simple particle balance model from equation (3), the slopes should differ by at least an order of magnitude between L-mode and H-mode due to differences in edge density ($n_e^{ped}/n_e^L \approx 2$), diffusivity ($D_L/D_H \approx 5$) and electron

temperature $c_s^H/c_s^L \approx \sqrt{10}$. However, although Δn_e in both confinement regimes scales linearly with ΔD_{OFL}, the change in slope between both confinement is far from an order of magnitude, i.e. the difference is slope is close to a factor of 3. There are several possible explanations to interpret the difference in slope between L-mode (MAST) and H-mode (DIII-D):

- Plasma response significantlly modifies the applied resonant magnetic field through screening and/or amplification. Assuming the amount of plasma response (δB) would be the same for all ΔD_{OFL} values, since they are all the consequence of an $n = 3$ spectrum in a similar background equilibrium, we can multiply ΔD_{OFL} with an amplification/screening factor A_i, resulting in a slope with gradient n/Dc_sA_i, with A_i being different for L-mode and H-mode, due to completely different pressure and rotation profiles.
- The changes in transport scale with ΔD_{OFL}, but not as 1 to 1. A scaling parameter $C_i \neq 1$ can change the slope effects and as shown in this paper, for example the changes in anomalous transport as a result of RMPs is ,vastly different for H-modes and L-mode, resulting in a different C_i for both experiments.
- More than one transport channel is altered an scales linearly with ΔD_{OFL}. Since both experiments are in a different confinement regime it is very likely that different transport channels will be important for each experiment. One example of such a possibility is the changes in turbulent transport, as shown in this paper. In L-mode (MAST) there is a clear increase in turbulent transport characteristics in the plasma edge, whereas in H-mode (DIII-D) the fluctuation levels actually decrease.

These are three possible explanations and further studies are needed to really understand the influence of RMP on particle transport. Future work needs to compare L- and H-mode on a single machine to eliminate some unknown factors that are part of a machine comparison.

4.4. Summary

Turbulence changes are seen in both experiments: in MAST L-modes, the normalized $\tilde{I}_{SAT}$ fluctuations in the edge increase with RMP-coil current after an initial threshold of 1 kA and there is no effect on the $E \times B$ shear inside $\Psi_N \leq 0.92$. In L-mode (MAST) the increase in fluctuations suggests that the density pump-out is the result of an increase in turbulent transport, once a threshold in RMP-coil current is exceeded. These changes in turbulent transport correspond well with the correlation of δn_e with ΔD_{OFL} for the L-modes (MAST) in figure 1. In DIII-D H-modes, an increase in $\tilde{n}/n$ at $\Psi_N \approx 0.88$ is correlated with lower $\omega_{E\times B}$, but this shear reduction is independent of applied RMP-coil current above the initial 4 kA level. At $\Psi_N \approx 0.95$, $\tilde{n}/n$ decreases with RMP-coil current. These results suggest that the mechanism for the increase in particle transport as a result of RMPs at the plasme edge in L-mode (MAST) is different from that in H-mode (DIII-D). In future work we will compare L- and H-mode data on DIII-D to eliminate some of the difference in parameters between MAST and DIII-D

Acknowledgments

This work was supported by the US Department of Energy under DE-FG02-05ER54809, DE-FG02-07ER54917, DE-FG02-89ER53296, and DE-FG02-08ER54999 and by the UK EPSRC and EURATOM. We would like to especially thank P. Peers.

[1] Evans T E *et al* 2004 *Phys. Rev. Lett.* **92** 235003

[2] Shimada M *et al* 2007 *Nucl. Fusion* **41** S1

[3] Snyder P B *et al* 2007 *Nucl. Fusion* **47** 961

[4] Mordijck S *et al* 2009 *J. Nucl. Mater.* **390-391** 299

[5] Evans T E *et al* 2006 *Nature Physics* **2** 419

[6] Moyer R A *et al* 2006 *Proc. 21st IAEA Fusion Energy Conference (Chengdu, China)* EX/93

[7] Kirk A *et al* 2010 *Nucl. Fusion* **50** 034008

[8] Schmitz O *et al* 2008 *Plasma Phys. Control. Fusion* **50** 124029

[9] Schmitz O *et al* 2009 *Phys. Rev. Lett.* **103** 165005

[10] Terry P W 2000 *Rev. Modern Phys.* **72** 1

[11] Burrell K H, Kaplan D H, Gohil P, Nilson D G, Groebner R J and Thomas D M 2001 *Rev. Sci. Instrum.* **72** 10228

[12] Yan Z *et al* 2010 *Proc. 23rd IAEA Fusion Energy Conference (Daejeon, Republic of Korea)* EXC/P305

[13] Moyer R A *et al* 2005 *Phys. Plasmas* **12** 056119

[14] Tamain P, Kirk A, Nardon E, Dudson B, Hnat B and the MAST team 2010 *Plasma Phys. Control. Fusion* **52** 075017

[15] Schmitz O *et al* 2009 *J. Nucl. Mater.* **390-391** 330

[16] Tokar M Z, Evans T E, Gupta A, Singh R, Kaw P and Wolf R C 2007 *Phys. Rev. Lett.* **98** 095001

[17] Yan L W and Evans T E 2007 *J. Nucl. Mater.* **363-365** 723

[18] Mordijck S, Owen L W, and Moyer R A 2010 *Nucl. Fusion* **50** .034006

[19] Evans T E *et al* 2008 *Nucl. Fusion* **48** 024002

[20] Rettig C L, Burns S, Philipona R, Peebles W A and Luhmann N C 1990 *Rev. Sci. Instrum.* **61** 3010

[21] Hahm T S and Burrell K H 1995 *Phys. Plasmas* **2** 1648

[22] McKee G, Ashley R, Durst R, Fonck R, Jakubowski M, Tritz K, Burrell K, Greeneld C and Robinson J 1999 *Rev. Sci. Instrum.* **70** 913

List of Figures

Fig. 1. (Color online) Density pump-out Δn_e as a function of the change in the weighted diffusion coefficient D_{OFL}, from equation (4) for H-mode (DIII-D) and L-mode (MAST) discharges. The H-mode results include the five different I-coil configurations and three different RMP spectra, two shapes and two distinct q_{95} values as indicated by the legend above the graph. Note that the L-mode values (diamonds) for ΔN_e are 10 times smaller than those for H-mode. The lines are linear regressions to the (DIII-D) H-mode (dashed) and MAST (L-mode) (solid) data sets respectively.

Fig. 2. (Color) Changes in radial profile of $E \times B$ shearomg rate as a function of RMP-coil current for DIII-D H-mode plasmas. $\omega_{E\times B}$ is calculated from the Hahm-Burrell formula for finite aspect ratio shaped plasmas [21]. All RMP discharges suppress ELMs with exception of the one at 4 kA, where ELMs are mitigated, but not suppressed. The two shaded areas (red and grey) are where we compare $E \times B$ shear with BES $\tilde{n}/n$ fluctuations.

Fig. 3. (Color online) $\tilde{n}/n$ (solid) and $\omega_{E\times B}$ (dashed) changes as a function of RMP-coil current for DIII-D H-mode discharges. The data are from two radial locations: $\Psi_N = 0.88$ (squares, corresponding to the grey band in figure 2) and $\Psi_N = 0.95$ (circles, corresponding to the red band in figure 2). The 0 kA and 4 kA discharges are ELMing; above 4 kA, the discharges are RMP ELM suppressed.

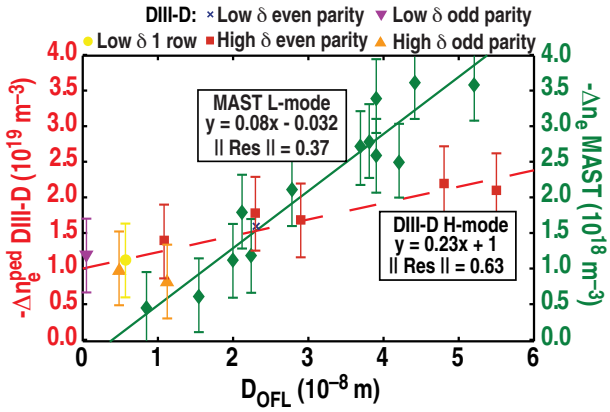

S. Mordijck Figure 1

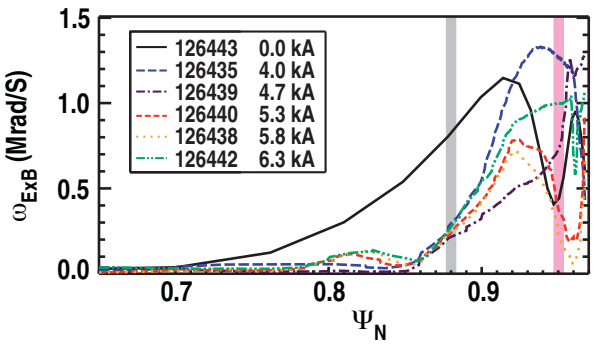

S. Mordijck

Figure 2

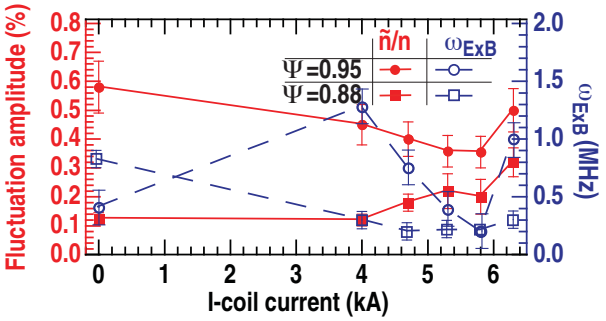

S. Mordijck

Figure 3